MULTIVARIATE ROUGH CLAIM PROCESSES: PROPERTIES AND ESTIMATION

Donatien Hainaut

LIDAM Discussion Paper ISBA
2022 / 02

ISBA
Voie du Roman Pays 20 - L1.04.01
B-1348 Louvain-la-Neuve
Email : lidam-library@uclouvain.be
https://uclouvain.be/en/research-institutes/lidam/isba/publication.html

Multivariate rough claim processes: properties and estimation

Donatien Hainaut*
UCLouvain, LIDAM-ISBA, Belgium

January 22, 2022

Abstract

This article studies a multivariate claim process with stochastic intensities driven by rough mean reverting diffusions. By construction, the dynamic of claim arrivals is induced by a fractional Brownian motion with a Hurst index, $H \in (0, \frac{1}{2})$. Therefore intensities have an infinite quadratic variation and are not semi-martingales. Nevertheless, we show that the moment generating function of the claim process admits a representation in terms of solutions of fractional differential equations. We next propose a procedure to filter the most likely sample path of rough intensities from time-series of claims. To illustrate this work, we estimate one and two dimensional rough models to time-series of cyber-attacks targeting medical and other services in the US from 2014 to 2018.

KEYWORDS: Fractional Brownian motion, rough volatility, Cox process.
JEL CODE : C5, G22

1 Introduction

The fractional Brownian motion (fBm) is comparable to a continuous fractal random walk. Unlike the regular Brownian motion (Bm), the fBm has dependent increments. This dependence is measured on a scale from zero to one by the Hurst index, $H \in (0, 1)$, named after hydrologist Harold Edwin Hurst for his work in the field of hydrology. The Hurst index describes the raggedness of the fBm sample path. A value of $1/2$ corresponds to the Bm with independent increments. A value of H greater (resp. lower) than $1/2$ corresponds to positive (resp. negative) correlation between increments.

Processes with $H > 1/2$ have a long term memory and sample paths are smoother than those of a Bm. When the Hurst index is below $1/2$, the fBm sample paths are "rough" and more chaotic than those of a Bm. Rough dynamics have recently received a great deal

*Postal address: Voie du Roman Pays 20, 1348 Louvain-la-Neuve (Belgium). E-mail to: donatien.hainaut(at)uclouvain.be

of attention in finance because they are consistent with empirical estimates of stock price volatility. In a seminal article, Gatheral et al. [13] propose a model for stock prices in which the volatility is driven by a fBm with $H < 1/2$. Jumarie [15] studies optimal asset allocation in a market driven by a fBm with $H < 1/2$. Bayer et al. [3] study option pricing under rough volatility. El Euch and Rosenbaum [10] and El Euch et al. [9] approximate the fBm by an integral with respect to a standard Bm in a Heston model and study option hedging strategies in this framework. El Euch and Rosenbaum [11] establish the characteristic of a rough Heston process. Abi Jaber et al. [1] show that rough models belong to the family of Affine Volterra processes. Abi Jaber and El Euch [2] characterize the Markovian and affine structure of the Volterra Heston model in terms of an infinite-dimensional forward process. Despite its attractiveness in finance, there are very few applications of rough dynamics to insurance. We can cite Dupret et al. [7] who value the impact of rough volatility on long-term annuities or Dupret and Hainaut [8] who study the performance of constant proportion portfolio insurance in a rough market.

This article contributes to the literature on rough models in several directions. To the best of our knowledge, this is the first work that investigates the properties of a multivariate claim process driven by multiple rough factors. From a methodological point of view, we express the joint characteristic function of claim processes in terms of solutions of fractional differential equations. Compared to the existing literature, we prove this result with an approach based on a discretization scheme similar to the one of Abi Jaber and El Euch [2] and Hainaut [14]. The characteristic function of claim processes present similarities with the one of the rough Heston model obtained by El Euch and Rosenbaum ([11]) by considering the limit of nearly unstable Hawkes processes. Our method for establishing such a result is nevertheless simple and novel since it is based on a discrete approximation of Riemann-Liouville derivatives. From an empirical point of view, this work develops a Monte-Carlo method to filter the sample path of rough intensities. Finally, the article proposes a case study on cyber risks.

The structure of this article is as follows. We start by presenting the rough claim process and remind its relation with the fractional Brownian motion. Since intensities of claim counting processes are not semi-martingales, we cannot rely on Itô calculus to study their properties. Nevertheless we show that rough factors admit an infinite dimensional Markov representation that we approximate by discretization in Section 3. In this discrete setting, the moment generating function (mgf) of claim processes is computable by solving backward ODE's. But this mgf does not admit any limit when the number of discretization steps increases. To tackle this issue, we express the approached mgf by the mean of forward ODE's. In Section 4, we reformulate them in term of discretized fractional derivatives. We find the mgf of claim processes by considering the limit. The calibration of a rough model is a challenging task since intensities of claims counting processes are not directly observable in practise. For this reason, we propose in Section 5, a procedure to filter their sample paths from claims time-series. The remainder of the article is devoted to a case study. In Section 6, we fit one and two dimensional rough models to time-series of cyber-attacks in the USA, targeting medical and other services from begin of 2014 to end of 2018. This dataset was investigated in papers of Bessy-Roland et al. [4]. In the last section, we compute the joint and marginal pdf's of claim processes by DFFT. This allows us to compare moments and percentiles to these of a standard Cox claim model.

2 A rough claim process?

The fBm has been introduced by Kolmogorov [16] and studied by Mandelbrot and van Ness [17]. Let $(\Omega, \mathcal{F}, \mathbb{P})$ denote a probability space and H, $0 \leq H \leq 1$, be referred to as the Hurst parameter. The stochastic process $\left(B_t^H\right)_{t\geq 0}$ defined on this probability space is a fractional Brownian motion (fBm) of order H if B_t^H is an $\mathcal{F}_t$-measurable Gaussian process such that $\mathbb{E}\left(B_t^H\right) = 0$ and for $t, s \in \mathbb{R}^+$, the autocovariance is:

$$\mathbb{E}\left(B_t^H B_s^H\right) \;= R_H(t,s) = \;\frac{1}{2}\left(t^{2H} + s^{2H} - |t-s|^{2H}\right) \tag{1}$$

It follows from (1) and from Kolmogorov's continuity criterion that the sample paths of B_t^H are continuous with probability one but nowhere differentiable. From the definition,we infer that the variance of the fBm is equal to

$$\mathbb{V}\left(B_t^H\right) \;=\; t^{2H}\,.$$

The fractional process is also self-similar i.e. the process $a^{-H}B_{at}^H$ has the same law as B_t^H for $a > 0$. The fBm can be rewritten as an integral with respect to a Bm, $(W_t)_{t\geq 0}$, which highlights the memory of the process:

$$B_t^H = \frac{1}{C_H}\left[\int_{-\infty}^0 \left((t-s)^{H-\frac{1}{2}} - (-s)^{H-\frac{1}{2}}\right) dW_s + \int_0^t (t-s)^{H-\frac{1}{2}}\, dW_s\right] \tag{2}$$

where C_H is function of the Hurst index. When $H < \frac{1}{2}$, it is natural to only consider the integral on the positive time axis when the Bm is not defined before time zero i.e. :

$$B_t^H \;\approx\; \frac{1}{\Gamma(\alpha)}\int_0^t (t-s)^{\alpha-1}\, dW_s \tag{3}$$

where $\alpha = H + 1/2 \in (\frac{1}{2}, 1)$. This approach was used by El Euch and Rosebaum ([11]) who propose a rough version of the Heston model. In this article, we consider claims processes for which the claim counts are Cox processes (or doubly stochastic processes) ruled by rough intensities based on the approximation (3) of the fractional Brownian motion.

We define m claim processes, noted $L_t^{(j)} = \sum_{k=1}^{N_t^{(j)}} J_k^{(j)}$, where $\left(N_t^{(j)}\right)_{t\geq 0}$ is a counting process for $j = 1, ..., m$. The claim sizes are distributed according to $J^{(j)}$, a random variable with expectation $\mathbb{E}(J^{(j)}) = \mu_j$ and a moment generating function $\varphi_j(\omega) = \mathbb{E}\left(e^{\omega J^{(j)}}\right)$ for $\omega \in \mathbb{C}^-$. The j^{th} counting process is a Cox process (See Cox [5]) with an intensity $\lambda_t^{(j)}$ that is a linear combination of rough processes $X_t^{(j)}$ for $j = 1, ..., p$ and $p \leq m$:

$$\lambda_t^{(j)} = \sum_{k=1}^{p} \phi_{j,k} X_t^{(k)} \quad , j = 1, ..., m\,, \tag{4}$$

where $(\phi_{j,k})_{j,k=1,...,p}$ are positive real coefficients. The $\left(X_t^{(j)}\right)_{j=1,...,p}$ are independent positive processes, ruled by the following dynamics:

$$X_t^{(j)} = X_0^{(j)} + \frac{1}{\Gamma(\alpha_j)}\int_0^t (t-s)^{\alpha_j-1}\kappa_j\left(\theta_j - X_s^{(j)}\right)ds \qquad (5)$$
$$+\frac{1}{\Gamma(\alpha_j)}\int_0^t (t-s)^{\alpha_j-1}\sqrt{X_s^{(j)}}\sigma_j dW_s^{(j)}\,,\; j=1,...,p$$

where $\alpha_j \in (\frac{1}{2},1)$, $\gamma,\kappa,\sigma \in \mathbb{R}^+$. This process is rough in the sense that its differential is not defined ($dX_t^{(j)} = \infty$). If $\alpha_j = 1$ for all $j = 1,...,p$, the $X_t^{(j)}$'s are Markov processes with a Cox-Ingersoll-Ross (CIR, [6]) dynamic:

$$dX_t^{(j)} = \kappa_j\left(\theta_j - X_t^{(j)}\right)dt + \sqrt{X_t^{(j)}}\sigma_j dW_t^{(j)}\,. \qquad (6)$$

This model will serves as benchmark in numerical illustrations. To lighten further developments, we respectively denote by Φ , the matrix of $(\phi_{j,k})_{j,k=1,...,p}$, by $(\mathcal{H}_t)_{t\geq 0}$ the filtration of $L_t^{(j)}$'s and by $(\mathcal{G}_t)_{t\geq 0}$ the filtration of $X_t^{(j)}$'s. The filtration $\mathcal{F}_t = \mathcal{H}_t \vee \mathcal{G}_t$ is the augmented filtration and gather information about all processes. We postulate that conditionally to the filtration $\mathcal{G}_t$, the multivariate counting process is a non-homogeneous Poisson process, i.e.

$$P(N_t^{(j)} = k|\mathcal{G}_t) \;=\; \frac{\left(\int_0^t \lambda_s^{(j)}ds\right)^k}{k!}\exp\left(-\int_0^t \lambda_s^{(j)}ds\right)\,.$$

$\left(N_t^{(j)}\right)_{t\geq 0}$ are Cox processes and the probability that no claim of type j is observed before time t is equal to $P(N_t^{(j)} = 0) = \mathbb{E}\left(\exp\left(-\int_0^t \lambda_s^{(j)}ds\right) \mid \mathcal{F}_0\right)$.

Since intensities are positive linear combinations of $\left(X_t^{(j)}\right)_{j=1,...,p}$, the proposed model manages exclusively positive correlations and then contagion between the different types of claims. This is happily the most common paradigm in practise. We could imagine to introduce negative correlation between Brownian motions $\left(W_t^{(j)}\right)_{j=1,...,p}$ driving the $\left(X_t^{(j)}\right)_{j=1,...,p}$. Unfortunately, the moment generating function of claim counting processes does not admit any closed-form expression in this case[1].

By construction, the processes $\left(X_t^{(j)}\right)_{j=1,...,p}$ are not Markov as their current values depend on their sample path up to time t. Nevertheless, we can reformulate them as an infinite dimensional Markov process. For this purpose, we rewrite the integrand in Eq. (5) as an

[1] Even when $\alpha = 1$, the model with correlation between $\left(W_t^{(j)}\right)_{j=1,...,p}$ is not analytically tractable because we are not in an affine framework anymore.

integral

$$
\begin{aligned}
(t-u)^{\alpha_j-1} &= \frac{1}{\Gamma(1-\alpha_j)}\int_0^{\infty}\frac{e^{-(t-u)\xi}}{\xi^{\alpha_j}}d\xi \\
&:= \int_0^{\infty} e^{-(t-u)\xi}\gamma_j(d\xi)\,,
\end{aligned}
$$

where $\gamma_j(d\xi) := \frac{\xi^{-\alpha_j}}{\Gamma(1-\alpha_j)}\,d\xi$ is a measure on $\mathbb{R}^+$. This observation allows us to reformulate the processes $X_t^{(j)}$ as an integral of an infinity of Ornstein-Uhlenbeck processes. We first use the Fubini theorem to develop the process X_t as an integral with respect to $\gamma_j(.)$:

$$
\begin{aligned}
X_t^{(j)} = X_0^{(j)} &+ \frac{1}{\Gamma(\alpha_j)}\int_0^{\infty}\int_0^t e^{-(t-s)\xi}\kappa_j\left(\theta_j - X_s^{(j)}\right)ds\,\gamma_j(d\xi) \\
&+ \frac{1}{\Gamma(\alpha_j)}\int_0^{\infty}\int_0^t e^{-(t-s)\xi}\sqrt{X_s^{(j)}}\sigma_j dW_s^{(j)}\,\gamma_j(d\xi).
\end{aligned}
$$

Next, we define the family of processes $Y_t^{(\xi,j)}$ indexed by $\xi \geq 0$ and $j = 1,...m$ that is:

$$
Y_t^{(\xi,j)} = \int_0^t e^{-(t-s)\xi}\kappa_j\left(\theta_j - X_s^{(j)}\right)ds + \int_0^t e^{-(t-s)\xi}\sqrt{X_s^{(j)}}\sigma_j dW_s^{(j)}\,.
$$

These processes are strictly positive, Markov and revert to $\frac{\kappa_j}{\xi}\left(\theta_j - X_t^{(j)}\right)$ with a speed ξ:

$$
dY_t^{(\xi,j)} \;=\; \xi\left(\frac{\kappa_j}{\xi}\left(\theta_j - X_t^{(j)}\right) - Y_t^{(\xi,j)}\right)dt + \sqrt{X_t}\,\sigma_j dW_t^{(j)}\,.
$$

The factor $X_t^{(j)}$ may finally be rewritten as an integral of $Y_t^{(\xi,j)}$ with respect to the measure $\gamma_j(.)$:

$$
X_t^{(j)} = X_0^{(j)} + \frac{1}{\Gamma(\alpha_j)}\int_0^{\infty} Y_t^{(\xi,j)}\,\gamma_j(d\xi)\,.
$$

which does not depend anymore upon information prior to t. This relation emphasizes that $\left(\lambda_t^{(j)}\right)_{j=1,\dots,m}$ and $\left(Y_t^{(\xi,j)}\right)_{\xi\in\mathbb{R}^+ j=1\dots m}$ form well an infinite dimensional Markov process.

The next sections focus on the joint moment generating function of $\int_0^t \boldsymbol{\lambda}_u du$ and $\boldsymbol{L}_t$ in $\mathbb{C}^{m-}$. Its determination requires a basic preliminary result presented in the next proposition.

Proposition 2.1. *For $\boldsymbol{\omega}_1$ and $\boldsymbol{\omega}_2 \in \mathbb{C}^{m-}$, the joint moment generating function of integrals of intensities and claim processes is given by:*

$$
\begin{aligned}
\mathbb{E}\left(e^{\boldsymbol{\omega}_1^\top\int_0^s\boldsymbol{\lambda}_u du+\boldsymbol{\omega}_2^\top\boldsymbol{L}_s}|\mathcal{F}_t\right) &= \exp\left(\boldsymbol{\omega}_1^\top\int_0^t\boldsymbol{\lambda}_u du + \boldsymbol{\omega}_2^\top\boldsymbol{L}_t\right)\times \\
&\prod_{j=1}^m\mathbb{E}\left(\exp\left(\left(\boldsymbol{\omega}_1+\boldsymbol{\varphi}(\boldsymbol{\omega}_2)-\mathbf{1}_m\right)^\top\Phi_{.,j}\int_t^s X_u^{(j)}du\right)|\mathcal{F}_t\right)\,,
\end{aligned}
\tag{7}
$$

where $\boldsymbol{\omega}_1+\boldsymbol{\varphi}(\boldsymbol{\omega}_2)-\mathbf{1}_m = \left(\varphi_j(\boldsymbol{\omega}_{2,j})-1\right)_{j=1,\dots,m}$ is a vector.

Proof We develop the mgf using nested expectations:

$$\mathbb{E}\left(e^{\boldsymbol{\omega}_1^\top \int_0^s \boldsymbol{\lambda}_u du+\boldsymbol{\omega}_2^\top \boldsymbol{L}_s}|\mathcal{F}_t\right) = \exp\left(\boldsymbol{\omega}_1^\top \int_0^t \boldsymbol{\lambda}_u du + \boldsymbol{\omega}_2^\top \boldsymbol{L}_t\right)$$
$$\times\, \mathbb{E}\left(e^{\boldsymbol{\omega}_1^\top \Phi \int_t^s \boldsymbol{X}_u du}\mathbb{E}\left(e^{\boldsymbol{\omega}_2^\top (\boldsymbol{L}_s-\boldsymbol{L}_t)}\,|\mathcal{F}_t \vee \mathcal{G}_s\right)|\mathcal{F}_t\right)\,.$$

Conditionally to the filtration $\mathcal{G}_s$, the claim processes are independent and the expectation in the right hand term of this equation may be rewritten as a product of expectations:

$$\mathbb{E}\left(e^{\boldsymbol{\omega}_2^\top (\boldsymbol{L}_s-\boldsymbol{L}_t)}\,|\mathcal{F}_t \vee \mathcal{G}_s\right) \;=\; \prod_{j=1}^{m} \mathbb{E}\left(e^{\omega_{2,j}\left(L_s^{(j)}-L_t^{(j)}\right)}|\mathcal{F}_t \vee \mathcal{G}_s\right)\,.$$

But $L_s^{(j)} - L_t^{(j)}|\mathcal{F}_t \vee \mathcal{G}_s$ is a compound Poisson process with a non-homogeneous intensity $\Phi_{j,.}\int_t^s \boldsymbol{X}_u du$. The moment generating function of $L_s^{(j)} - L_t^{(j)}$ is then given by

$$\mathbb{E}\left(e^{\omega_{2,j}\left(L_s^{(j)}-L_t^{(j)}\right)}|\mathcal{F}_t \vee \mathcal{G}_s\right) \;=\; \exp\left(\left(\varphi_j(\omega_{2,j})-1\right)\Phi_{j,.}\int_t^s \boldsymbol{X}_u du\right)\,.$$

and we retrieve Equation (7).

■

Determining the joint mgf of $\int_0^t \boldsymbol{\lambda}_u du$ and $\boldsymbol{L}_t$ in $\mathbb{C}^{m-}$, requires to find the mgf's of rough factor integrals for $j = 1, ..., p$ which is a challenging task. We can draw a parallel between factors $\left(X_t^{(j)}\right)_{t\geq 0}$ and the stochastic volatility of the rough Heston model, for which El Euch and Rosenbaum ([11]) found the mgf by considering the limit of nearly unstable Hawkes processes. Nevertheless, this mgf of stock prices does not help us in the context of this article. An alternative consists to reformulate $X_t^{(j)}$ and $\int_0^t X_u^{(j)} du$ as a Volterra system and to calculate the resolvent of the memory kernel. The mgf's of $X_t^{(j)}$ can then be obtained by solving Ricatti Volterra equations, as detailed in Abi Jaber et al. [1]. In this work, we opt for a simpler method that consists to approximate rough factors by discretization in a similar way to Abi Jaber and El Euch ([2]). The novelty of our approach consists to show that the mgf's of integrals of approximated rough factors may be rewritten in terms of discretized fractional derivatives.

3 Discrete approximation of the rough model

Instead of considering an infinity of processes $\left(Y_t^{(\xi,j)}\right)_{t\geq 0}$, we approach the model with a finite number of equivalent processes. This presents for main advantage that we can rely on the Itô's calculus to study features of the claim process. The key step consists to approach $\gamma_j(.)$ by a discrete measure with a finite numbers of atoms. For this purpose we consider a partition $\mathcal{E}^{(n)} := \{0 < \xi_0^{(n)} < \xi_1^{(n)} < ... < \xi_n^{(n)} < \infty\}$. The mid point of each interval $(\xi_i^{(n)}, \xi_{i+1}^{(n)})$ is

$$b_{k+1} \;=\; \frac{\xi_k^{(n)}+\xi_{k+1}^{(n)}}{2} \tag{8}$$

and the mass of corresponding atoms is defined as the measure of intervals of the partition:

$$m_{k+1}^{(j)} = \int_{\xi_k^{(n)}}^{\xi_{k+1}^{(n)}} d\gamma_j(z) = \frac{\left(\left(\xi_{k+1}^{(n)}\right)^{1-\alpha_j} - \left(\xi_k^{(n)}\right)^{1-\alpha_j}\right)}{\Gamma(1-\alpha_j)(1-\alpha_j)}\,, \tag{9}$$

for $k = 0, ..., n-1$. The discrete measure for a partition of size n is defined as follows

$$\bar{\gamma}_j(z) = \sum_{k=1}^{n} m_k^{(j)} \delta_{b_k}(z)\,, \tag{10}$$

where $\delta_{b_k}(z)$ is the Dirac measure located at point b_k. We consider that the following assumption holds for the partition $\mathcal{E}^{(n)}$:

- $\xi_0^{(n)} \to 0$ and $\xi_n^{(n)} \to \infty$ when $n \to \infty$.
- $\max |\xi_{i+1}^{(n)} - \xi_i^{(n)}| \to 0$ when $n \to \infty$.
- $\mathcal{E}^{(n)} \subset \mathcal{E}^{(n+1)}$.

In this case, for any function $f(.)$ integrable with respect to $\gamma_j(.)$, we have that $\lim_{n\to\infty} \int_0^\infty f(z)\, d\bar{\gamma}_j(z) = \int_0^\infty f(z)\, d\gamma_j(z)$. To lighten further developments, we adopt the following notations $Y_t^{(j,k)} := Y_t^{(b_k,j)}$ for $k = 1, ..., n$ where

$$Y_t^{(j,k)} = \int_0^t e^{-(t-s)b_k} \kappa_j \left(\theta_j - \bar{X}_s^{(j)}\right) ds + \int_0^t e^{-(t-s)b_k} \sqrt{\bar{X}_s^{(j)}}\, \sigma_j dW_s^{(j)}\,.$$

and $\bar{X}_t^{(j)} = X_0^{(j)} + \frac{1}{\Gamma(\alpha_j)} \sum_{k=1}^{n} Y_t^{(j,k)} m_k^{(j)}$ is the process approximating $X_t^{(j)}$. We also write $\bar{\lambda}_t^{(j)} = \Phi_{j,.} \bar{\boldsymbol{X}}_t$ where $\bar{\boldsymbol{X}}_t$ is the $m-$vector of $\bar{X}_t^{(j)}$. The differential of this process is

$$dY_t^{(j,k)} = \left(\kappa_j \left(\theta_j - \bar{X}_t^{(j)}\right) - b_k Y_t^{(j,k)}\right) dt + \sqrt{\bar{X}_t^{(j)}}\, \sigma_j dW_t^{(j)}\,, \tag{11}$$

for $k = 1, ..., n$ and $j = 1, ..., m$. On the other hand, the dynamics of rough processes are approached by

$$\begin{aligned} d\bar{X}_t^{(j)} &= \frac{1}{\Gamma(\alpha_j)} \sum_{k=1}^{n} m_k^{(j)} \left(\kappa_j \left(\theta_j - \bar{X}_t^{(j)}\right) - b_k Y_t^{(j,k)}\right) dt \\ &\quad + \frac{\sqrt{\bar{X}_t^{(j)}}}{\Gamma(\alpha_j)} \sum_{k=1}^{n} m_k^{(j)} \sigma_j dW_t^{(j)}\,. \end{aligned} \tag{12}$$

The discretized version of the claim process is noted $\left(\bar{L}_t^{(j)}\right)_{t\geq 0}$ and its vector $\bar{\boldsymbol{L}}_t$ and $\bar{\boldsymbol{\lambda}}_t$ is the m-vector of intensities. The next proposition presents the moment generating function (mgf) of $\int_0^t \bar{\boldsymbol{\lambda}}_u du$ and $\bar{\boldsymbol{L}}_t$ on $\mathbb{C}^{m-}$.

Proposition 3.1. *For $\boldsymbol{\omega}_1$ and $\boldsymbol{\omega}_2 \in \mathbb{C}^{m-}$, the joint moment generating function of integrals of intensities and claim processes is given by:*

$$\mathbb{E}\left(e^{\boldsymbol{\omega}_1^\top \int_0^s \bar{\boldsymbol{\lambda}}_u du + \boldsymbol{\omega}_2^\top \bar{\boldsymbol{L}}_s} | \mathcal{F}_t\right) = \exp\left(\boldsymbol{\omega}_1^\top \int_0^t \bar{\boldsymbol{\lambda}}_u du + \boldsymbol{\omega}_2^\top \bar{\boldsymbol{L}}_t\right) \times \prod_{j=1}^m \exp\left(a_j(t,s) + c_j(t,s)\bar{X}_t^{(j)} - \sum_{k=1}^n d_{j,k}(t,s) Y_t^{(j,k)}\right), \tag{13}$$

where

$$d_{j,k}(t,s) \quad = \quad m_k^{(j)} b_k \int_t^s e^{-b_k(u-t)} \frac{c_j(u,s)}{\Gamma(\alpha_j)} \, du\,, \tag{14}$$

and functions $a_j(t,s)$ and $c_j(t,s)$ solves a backward system of ordinary differential equations:

$$\partial_t a_j(t,s) = -\frac{\kappa_j \theta_j}{\Gamma(\alpha_j)} \sum_{k=1}^n m_k^{(j)} \left(c_j(t,s) - b_k \int_t^s e^{-b_k(u-t)} c_j(u,s)\, du\right), \tag{15}$$

$$\begin{aligned}\partial_t c_j(t,s) = &-\left(\boldsymbol{\omega}_1 + \boldsymbol{\varphi}(\boldsymbol{\omega}_2) - \mathbf{1}_m\right)^\top \Phi_{.,j} \\ &+ \frac{\kappa_j}{\Gamma(\alpha_j)} \sum_{k=1}^n m_k^{(j)} \left(c_j(t,s) - b_k \int_t^s e^{-b_k(u-t)} c_j(u,s)\, du\right) \\ &- \frac{1}{2} \frac{\sigma_j^2}{\Gamma(\alpha_j)^2} \left(\sum_{k=1}^n m_k^{(j)} \left(c_j(t,s) - b_k \int_t^s e^{-b_k(u-t)} c_j(u,s)\, du\right)\right)^2,\end{aligned} \tag{16}$$

with the terminal conditions $a(s,s) = 0$ and $c_j(s,s) = 0$ for $j = 1, ..., m$.

Proof From Proposition 2.1, we immediately infer that

$$\mathbb{E}\left(e^{\boldsymbol{\omega}_1^\top \int_0^s \bar{\boldsymbol{\lambda}}_u du + \boldsymbol{\omega}_2^\top \bar{\boldsymbol{L}}_s} | \mathcal{F}_t\right) = \exp\left(\boldsymbol{\omega}_1^\top \int_0^t \bar{\boldsymbol{\lambda}}_u du + \boldsymbol{\omega}_2^\top \bar{\boldsymbol{L}}_t\right) \times \prod_{j=1}^m \mathbb{E}\left(\exp\left(\left(\boldsymbol{\omega}_1 + \boldsymbol{\varphi}(\boldsymbol{\omega}_2) - \mathbf{1}_m\right)^\top \Phi_{.,j} \int_t^s \bar{X}_u^{(j)} du\right) | \mathcal{F}_t\right),$$

and the remainder of the proof focuses on the calculation of $\mathbb{E}\left(\exp\left(\omega \int_t^s \bar{X}_u^{(j)} du\right) | \mathcal{F}_t\right)$. This mgf is a function of several state variables, that is denoted by $f\left(t, \bar{X}_t^{(j)}, \left(Y_t^{(j,k)}\right)_{k=1,\ldots,n}\right)$. As $f(.)$ is a conditional expectation, it satisfies the following partial differential equation:

$$\begin{aligned}-\omega \bar{X}_t^{(j)} f = {}& \partial_t f + \partial_{\bar{X}^{(j)}} f \frac{1}{\Gamma(\alpha_j)} \sum_{k=1}^n m_k^{(j)} \left(\kappa_j \left(\theta_j - \bar{X}_t^{(j)}\right) - b_k Y_t^{(j,k)}\right) + \\ & \sum_{k=1}^n \partial_{Y^{(j,k)}} f \left(\kappa_j \left(\theta_j - \bar{X}_t^{(j)}\right) - b_k Y_t^{(j,k)}\right) + \frac{1}{2} X_t^{(j)} \sigma_j^2 \sum_{k_1=1,k_2=1}^n \partial^2_{Y^{(j,k_1)} Y^{(j,k_2)}} f \\ & + \bar{X}_t^{(j)} \frac{\sigma_j^2 \sum_{l=1}^n m_l^{(j)}}{\Gamma(\alpha_j)} \sum_{k=1}^n \partial^2_{\bar{X}^{(j)} Y^{(j,k)}} f + \frac{1}{2} \bar{X}_t^{(j)} \frac{\sigma_j^2 \left(\sum_{l=1}^n m_l^{(j)}\right)^2}{\Gamma(\alpha_j)^2} \partial^2_{\bar{X}^{(j)} \bar{X}^{(j)}} f\,.\end{aligned} \tag{17}$$

By construction, the model has an affine structure, we consider the ansatz that $f(.)$ is an exponential function of the form:

$$f = \exp(a_j(t,s) + c_j(t,s)\bar{X}_t^{(j)} - \sum_{k=1}^{n} d_{j,k}(t,s) Y_t^{(j,k)}) ,$$

where $a_j(t,s)$, $c_j(t,s)$ and $d_{j,k}(t,s)$ are C_1 functions, for $j = 1, ..., m$ and $k = 1, ..., n$. Replacing the partial derivatives of f, into Equation (17) and regrouping and cancelling terms multiplying $\bar{X}_t^{(j)}$ and $Y_t^{(j,k)}$ allows us to infer that functions $a_j(.,.)$, $c_j(.,.)$ and $d_{j,k}(.,.)$ solve a system of ordinary differential equations:

$$\begin{aligned}
0 &= \partial_t a_j(t,s) + \kappa_j \theta_j \sum_{k=1}^{n} \left(\frac{c_j(t,s)\, m_k^{(j)}}{\Gamma(\alpha_j)} - d_{j,k}(t,s) \right) \\
0 &= \partial_t c_j(t,s) + \omega - \kappa_j \sum_{k=1}^{n} \left(\frac{c_j(t,s)}{\Gamma(\alpha_j)} m_k^{(j)} - d_{j,k}(t,s) \right) + \\
&\quad + \frac{1}{2}\sigma_j^2 \left(\sum_{k=1}^{n} \left(\frac{m_k^{(j)}}{\Gamma(\alpha_j)} c_j(t,s) - d_{j,k}(t,s) \right) \right)^2 \\
0 &= -\partial_t d_{j,k}(t,s) - \frac{c_j(t,s)}{\Gamma(\alpha_j)} m_k^{(j)} b_k + d_{j,k}(t,s)\, b_k
\end{aligned}$$

With the terminal condition, $d_{j,k} = 0$, we infer that $d_{j,k}(t,s)$ is proportional to an integral of $c_j(.,.)$ and given by Equation (14) whereas a_j and c_j solve Equations (15) and (16).

■

We infer in the next corollary that functions $c_j(t,s)$ are homegeneous in the sense they only depend on $(s-t)$. This property is needed in later developments.

Corollary 3.2. *For any $s, s' \in \mathbb{R}^+$ and $v \in \mathbb{R}^+$, the following equality holds*

$$c_j(s-v, s) = c_j(s'-v, s') \quad j = 1, ..., p \tag{18}$$

Proof By definition this equality is true for $v = 0$, $c_j(s,s) = c_j(s',s') = 0$. Let us then assume that the property (18) holds for all $l \in [0, v]$ where $0 < v \le s$. From Equations (16) and (14), we infer that

$$\begin{aligned}
\frac{\partial c_j(s-v,s)}{\partial v} &= - \left. \frac{\partial c_j(t,s)}{\partial t} \right|_{t=s-v} = (\boldsymbol{\omega}_1 + \boldsymbol{\varphi}(\boldsymbol{\omega}_2) - \mathbf{1}_m)^\top \Phi_{.,j} \\
&- \frac{\kappa_j}{\Gamma(\alpha_j)} \sum_{k=1}^{n} m_k^{(j)} \left(c_j(s-v,s) - b_k \int_{s-v}^{s} e^{-b_k(u-(s-v))} c_j(u,s)\, du \right) \\
&+ \frac{1}{2} \frac{\sigma_j^2}{\Gamma(\alpha_j)^2} \left(\sum_{k=1}^{n} m_k^{(j)} \left(c_j(s-v,s) - b_k \int_{s-v}^{s} e^{-b_k(u-(s-v))} c_j(u,s)\, du \right) \right)^2 .
\end{aligned}$$

We rewrite the integrals in the previous equation using the change of variable $u = s - l$,

$$\int_{s-v}^{s} e^{-b_k(u-(s-v))} c_j(u,s)\,du \;=\; \int_0^v e^{-b_k(v-l)} c_j(s-l,s)\,dl$$

Since $c_j(s-l,s) = c_j(s'-l,s')$ for all $l \in [0,v]$, we infer that

$$\frac{\partial c_j(s-v,s)}{\partial v} = \frac{\partial c_j(s'-v,s')}{\partial v},$$

and conclude that the equality (18) holds for $v + dv$.

■

We may think to infer the moment generating function in the continuous case as defined by Equation (5), by considering the limit of the system in Proposition 3.1 when the granularity of the partition tends to infinity. Nevertheless, this approach fails because the limit of the sum of $m_k^{(j)}$ is not defined:

$$\lim_{n\to\infty} \sum_{k=1}^{n} m_k^{(j)} \;=\; \int_0^\infty \gamma^{(j)}(d\xi) = \infty\,.$$

In order to find the expression of the mgf when $n \to \infty$, we first show that it is computable by solving a system of forward fractional differential equations. Next, we will prove that the limit of this system when the granularity of the partition tends to infinity, can be reformulated as a function of Riemann-Liouville derivatives.

Proposition 3.3. *For ω_1 and $\omega_2 \in \mathbb{C}^{m-}$, the joint moment generating function of claim processes and integrals of intensities is given by*

$$\mathbb{E}\left(e^{\boldsymbol{\omega}_1^\top \int_0^s \bar{\boldsymbol{\lambda}}_u du + \boldsymbol{\omega}_2^\top \bar{\boldsymbol{L}}_s} | \mathcal{F}_t\right) = \exp\left(\boldsymbol{\omega}_1^\top \int_0^t \bar{\boldsymbol{\lambda}}_u du + \boldsymbol{\omega}_2^\top \bar{\boldsymbol{L}}_t\right) \times$$
$$\prod_{j=1}^{m} \exp\left(a_j(t,s) + c_j(t,s)\bar{X}_t^{(j)} - \sum_{k=1}^{n} d_{j,k}(t,s) Y_t^{(j,k)}\right)$$

where $d_{j,k}(t,s)$ is given by Equation (14) and functions $a_j(t,s)$ and $c_j(t,s)$ solves a forward system of ordinary differential equations:

$$\partial_s a_j(t,s) = \frac{\kappa_j \theta_j}{\Gamma(\alpha_j)} \sum_{k=1}^{n} m_k^{(j)} \left(\partial_s \int_t^s e^{-b_k(u-t)}\, c_j(u,s)\,du\right) \tag{19}$$

$$\begin{aligned}\partial_s c_j(t,s) &= \left(\boldsymbol{\omega}_1 + \boldsymbol{\varphi}(\boldsymbol{\omega}_2) - \mathbf{1}_m\right)^\top \Phi_{.,j} \\ &- \frac{\kappa_j}{\Gamma(\alpha_j)} \sum_{k=1}^{n} m_k^{(j)} \left(\partial_s \int_t^s e^{-b_k(u-t)} c_j(u,s)\,du\right) \\ &+ \frac{1}{2}\frac{\sigma_j^2}{\Gamma(\alpha_j)^2} \left(\sum_{k=1}^{n} m_k^{(j)} \left(\partial_s \int_t^s e^{-b_k(u-t)} c_j(u,s)\,du\right)\right)^2\end{aligned} \tag{20}$$

with the initial conditions $a(t,t) = 0$ and $c_j(t,t) = 0$ for $j = 1, \dots, m$.

Proof From Proposition 3.1 and as $a_j(s,s)=0$, we infer that the function $a_j(t,s)$ is equal to

$$\begin{aligned}
a_j(t,s) &= \frac{\kappa_j\theta_j}{\Gamma(\alpha_j)}\sum_{k=1}^{n} m_k^{(j)}\left(\int_t^s c_j(u,s)du - b_k\int_t^s\int_u^s e^{-b_k(v-u)}c_j(v,s)dv\,du\right)\\
&= \frac{\kappa_j\theta_j}{\Gamma(\alpha_j)}\sum_{k=1}^{n} m_k^{(j)}\left(\int_t^s c_j(u,s)du - b_k\int_t^s \frac{1}{b_k}\left(1-e^{-b_k(v-t)}\right) c_j(v,s)\,dv\right)\\
&= \frac{\kappa_j\theta_j}{\Gamma(\alpha_j)}\sum_{k=1}^{n} m_k^{(j)}\left(\int_t^s e^{-b_k(u-t)}\,c_j(u,s)\,du\right).
\end{aligned}$$

We then retrieve Equation (19) by deriving this expression with respect to s. On the other hand, integrating Equation (16) leads to the following expression for the function $c_j(0,s)$:

$$\begin{aligned}
c_j(t,s) &= (\boldsymbol{\omega}_1+\boldsymbol{\varphi}(\boldsymbol{\omega}_2)-\mathbf{1}_m)^\top\,\Phi_{.,j}\,(s-t) - \frac{\kappa_j}{\Gamma(\alpha_j)}\sum_{k=1}^{n} m_k^{(j)}\int_t^s e^{-b_k(u-t)}\,c_j(u,s)\,du\\
&+\frac{1}{2}\frac{\sigma_j^2}{\Gamma(\alpha_j)^2}\int_t^s\left(\sum_{k=1}^{n} m_k^{(j)}\left(c_j(v,s)-b_k\int_v^s e^{-b_k(u-v)}c_j(u,s)du\right)\right)^2 dv\,.
\end{aligned}$$

If we remember that $c(s,s)=0$, deriving this last expression with respect to s leads to

$$\begin{aligned}
\partial_s c_j(0,s) &= (\boldsymbol{\omega}_1+\boldsymbol{\varphi}(\boldsymbol{\omega}_2)-\mathbf{1}_m)^\top\,\Phi_{.,j} - \frac{\kappa_j}{\Gamma(\alpha_j)}\sum_{k=1}^{n} m_k^{(j)}\left[\partial_s\int_t^s e^{-b_k(u-t)}\,c_j(u,s)\,du\right] \qquad (21)\\
&+\frac{\sigma_j^2}{2\Gamma(\alpha_j)^2}\partial_s\int_t^s\left(\sum_{k=1}^{n} m_k^{(j)}\left(c_j(v,s)-b_k\int_v^s e^{-b_k(u-v)}c_j(u,s)du\right)\right)^2 dv
\end{aligned}$$

and the derivative in the last term of this equation is developped as the following sum:

$$\begin{aligned}
&\frac{1}{2}\partial_s\int_t^s\left(\sum_{k=1}^{n} m_k^{(j)}\left(c_j(v,s)-b_k\int_v^s e^{-b_k(u-v)}c_j(u,s)du\right)\right)^2 dv \qquad (22)\\
&=\sum_{k=1}^{n}\sum_{l=1}^{n} m_k^{(j)}m_l^{(j)}\int_t^s\left(c_j(v,s)\partial_s c_j(v,s)\right)dv\\
&-\sum_{k=1}^{n}\sum_{l=1}^{n} m_k^{(j)}m_l^{(j)}b_l\int_t^s\left(c_j(v,s)\int_v^s e^{-b_l(u-v)}\partial_s c_j(u,s)du\right)dv\\
&-\sum_{k=1}^{n}\sum_{l=1}^{n} m_k^{(j)}m_l^{(j)}b_k\int_t^s\left(\partial_s c_j(v,s)\int_v^s e^{-b_k(u-v)}c_j(u,s)du\right)dv\\
&+\sum_{k=1}^{n}\sum_{l=1}^{n} m_k^{(j)}m_l^{(j)}b_k b_l\int_t^s\left(\int_v^s e^{-b_k(u-v)}c_j(u,s)du\int_v^s e^{-b_l(u-v)}\partial_s c_j(u,s)du\right)dv\,.
\end{aligned}$$

As $c_j(v,s)\partial_s c_j(v,s)=\frac{1}{2}\partial_s c_j(v,s)^2$, the first term in this last equation is rewritten as

$$\int_t^s\left(c_j(v,s)\partial_s c_j(v,s)\right)dv = \frac{1}{2}\partial_s\int_t^s c_j(v,s)^2 dv\,.$$

On the other hand, as $c_j(s,s)=0$, the sum of the second and third terms in Equation (22) are gathered as follows:

$$
\begin{aligned}
&\sum_{k=1}^{n}\sum_{l=1}^{n} m_k^{(j)} m_l^{(j)} b_l \int_t^s \left(c_j(v,s) \int_v^s e^{-b_l(u-v)} \partial_s c_j(u,s) du \right) dv \\
&+ \sum_{k=1}^{n}\sum_{l=1}^{n} m_k^{(j)} m_l^{(j)} b_k \int_t^s \left(\partial_s c_j(v,s) \int_v^s e^{-b_k(u-v)} c_j(u,s) du \right) dv \\
&= \sum_{k=1}^{n}\sum_{l=1}^{n} m_k^{(j)} m_l^{(j)}\, b_k \partial_s \int_t^s \left(c_j(v,s) \int_v^s e^{-b_k(u-v)} c_j(u,s) du \right) dv\,.
\end{aligned}
$$

As $\partial_s \int_v^s e^{-b_l(u-v)} c_j(u,s)du = \int_v^s e^{-b_l(u-v)} \partial_s c_j(u,s)du$, we rewrite the last term of Equation (22) as follows:

$$
\begin{aligned}
&\sum_{k=1}^{n}\sum_{l=1}^{n} m_k^{(j)} m_l^{(j)} b_k b_l \int_t^s \left(\int_v^s e^{-b_k(u-v)} c_j(u,s) du \int_v^s e^{-b_l(u-v)} \partial_s c_j(u,s) du \right) dv = \\
&\frac{1}{2}\sum_{k=1}^{n}\sum_{l=1}^{n} m_k^{(j)} m_l^{(j)} b_k b_l \partial_s \int_t^s \left(\int_v^s e^{-b_k(u-v)} c_j(u,s) du \int_v^s e^{-b_l(u-v)} c_j(u,s) du \right) dv\,.
\end{aligned}
$$

We finally obtain that

$$
\begin{aligned}
&\frac{1}{2}\partial_s \int_t^s \left(\sum_{k=1}^{n} m_k^{(j)} \left(c_j(v,s) - b_k \int_v^s e^{-b_k(u-v)} c_j(u,s) du \right) \right)^2 dv \qquad (23) \\
&= \frac{1}{2}\left(\sum_{k=1}^{n} m_k^{(j)} \partial_s \int_t^s \left(c_j(v,s) - b_k \int_v^s e^{-b_k(u-v)} c_j(u,s) du \right) dv \right)^2 \\
&= \frac{1}{2}\left(\sum_{k=1}^{n} m_k^{(j)} \partial_s \int_t^s e^{-b_k(u-t)}\, c_j(u,s)\, du \right)^2 .
\end{aligned}
$$

Injecting this result into Equation (21) leads to the expression (20).

■

We now dispose of all intermediate results to infer the joint mgf of $\int_0^s \boldsymbol{\lambda}_u du$ and $\boldsymbol{L}_s$ by studying the limit of the system of ODE's (19) and (20) when the size of the partition converges to infinity.

4 Link with fractional calculus

We show in this section that equations (19) and (20) can be reformulated as fractional differential equations when the granularity of the partition $\mathcal{E}^{(n)}$ tends to infinity. For this purpose, let us recall that the left Riemann-Liouville integral for $\alpha \in (0,1]$ is defined for any integrable functions $f(.)$ by:

$$
I^{\alpha} f(t) = \frac{1}{\Gamma(\alpha)} \int_0^t (t-u)^{\alpha-1} f(u)\, du\,.
$$

By construction, $I^\alpha f(t)$ corresponds to the classical Riemann integral when $\alpha = 1$. The left Riemann-Liouville derivative, denoted by $D^{1-\alpha} f(t)$, is the derivative of $I^\alpha f(t)$:

$$D^{1-\alpha} f(t) = \frac{dI^\alpha f(t)}{dt} = \frac{1}{\Gamma(\alpha)} \frac{d}{dt} \int_0^t \frac{f(u)}{(t-u)^{1-\alpha}}\, du\,.$$

If we remember that $(t-u)^{\alpha-1}$ can be rewritten as an integral with respect to a measure $\gamma(d\xi)$:

$$(t-u)^{\alpha-1} = \frac{1}{\Gamma(1-\alpha)} \int_0^\infty \frac{e^{-(t-u)\xi}}{\xi^\alpha} d\xi := \int_0^\infty e^{-(t-u)\xi} \gamma(d\xi)\,,$$

we can develop the left fractional derivative as follows:

$$\begin{aligned}
D^{1-\alpha} f(t) &= \frac{1}{\Gamma(\alpha)} \frac{d}{dt} \int_0^t \frac{f(u)}{(t-u)^{1-\alpha}}\, du \\
&= \frac{1}{\Gamma(\alpha)} \int_0^\infty \frac{d}{dt} \int_0^t \frac{e^{-(t-u)\xi}}{\Gamma(1-\alpha)\xi^\alpha} f(u)\, du\, d\xi \\
&= \frac{1}{\Gamma(\alpha)} \int_0^\infty \left(f(t) - \xi \int_0^t e^{-(t-u)\xi} f(u)\, du \right) \gamma(d\xi) \\
&= \frac{1}{\Gamma(\alpha)} \int_0^\infty \left(\frac{d}{dt} \int_0^t e^{-(t-u)\xi} f(u)\, du \right) \gamma(d\xi)
\end{aligned}$$

If we replace the measure $\gamma(.)$ by its discrete equivalent $\bar{\gamma}(.)$ on a partition $\mathcal{E}^{(n)}$, as defined by equations (9) and (10), the fractional derivative is approached by :

$$D^{1-\alpha,(n)} f(t) = \frac{1}{\Gamma(\alpha)} \sum_{k=0}^{n} m_k \left(\frac{d}{dt} \int_0^t e^{-(t-u)b_k} f(u)\, du \right)\,. \tag{24}$$

If we compare this last expression with equations (19) and (20), we observe similar patterns. This conclusion is the starting point of the proof of the next result.

Proposition 4.1. *Let us denote by $\psi_j(s)$, the solution of the fractional forward ODE:*

$$D^{\alpha_j} \psi_j(s) = (\boldsymbol{\omega}_1 + \boldsymbol{\varphi}(\boldsymbol{\omega}_2) - \mathbf{1}_m)^\top \Phi_{.,j} - \kappa_j \psi_j(s) + \frac{\sigma_j^2}{2} \psi_j(s)^2\,, \tag{25}$$

with the initial condition $\psi_j(0) = 0$ for $j = 1, ..., m$. The joint moment generating function of $\int_0^s \boldsymbol{\lambda}_u du$ and $\boldsymbol{L}_s$, conditionally to the filtration at time $t = 0$ is

$$\mathbb{E}\left(e^{\boldsymbol{\omega}_1^\top \int_0^s \boldsymbol{\lambda}_u du + \boldsymbol{\omega}_2^\top \boldsymbol{L}_s} | \mathcal{F}_0 \right) = \prod_{j=1}^{m} \exp\left(a_j(0,s) + c_j(0,s) X_0^{(j)} \right)\,, \tag{26}$$

where $c_j(0,s) = I^{1-\alpha_j} \psi_j(s)$ and $a_j(0,s)$ solves the forward ordinary differential equation

$$\partial_s a_j(0,s) = \kappa_j \theta_j\, \psi_j(s)\,, \tag{27}$$

with the initial conditions $a_j(0,0) = 0$.

Proof From property (18), we know that $c_j(t,s)$ is an homogeneous function of $v=(s-t)$. Therefore we denote it by $\tilde{c}_j(v)=c_j(s-v,s)$. If we perform the change of variable $v=s-u$, we have that

$$\int_0^s e^{-b_k u} c_j(u,s)\,du \;=\; \int_0^s e^{-b_k(s-v)}\tilde{c}_j(v)\,dv\,,$$

and the left term in Equation (19) can be reformulated as a discretized fractional derivative of $\tilde{c}_j(.)$:

$$\frac{1}{\Gamma(\alpha_j)}\sum_{k=1}^{n} m_k^{(j)}\partial_s\int_0^s e^{-b_k u}\,c_j(u,s)\,du = D^{1-\alpha_j,(n)}\tilde{c}_j(s)\,.$$

The derivative of the function $a_j(0,s)$ depends upon this discretized fractional derivative,

$$\partial_s a_j(0,s) \;=\; \kappa_j\theta_j\left(D^{1-\alpha_j,(n)}\tilde{c}_j(s)\right)\,. \tag{28}$$

In a similar manner, the derivative of $c_j(0,s)$ with respect to the considered time horizon becomes:

$$\begin{aligned}\partial_s c_j(0,s) &= (\boldsymbol{\omega}_1+\boldsymbol{\varphi}(\boldsymbol{\omega}_2)-\mathbf{1}_m)^\top\,\Phi_{.,j}-\kappa_j\left(D^{1-\alpha_j,(n)}\tilde{c}_j(s)\right) \\ &\quad+\frac{\sigma_j^2}{2}\left(D^{1-\alpha_j,(n)}\tilde{c}_j(s)\right)^2\,.\end{aligned} \tag{29}$$

When the size of the partition $\mathcal{E}^{(n)}$ growths to infinity, the limit of Equations (28) and (29) are given by:

$$\begin{aligned}\partial_s a_j(0,s) &= \kappa_j\theta_j\left(D^{1-\alpha_j}\tilde{c}_j(s)\right)\,,\\ \partial_s c_j(0,s) &= (\boldsymbol{\omega}_1+\boldsymbol{\varphi}(\boldsymbol{\omega}_2)-\mathbf{1}_m)^\top\,\Phi_{.,j}-\kappa_j\left(D^{1-\alpha_j}\tilde{c}_j(s)\right)\\ &\quad+\frac{\sigma_j^2}{2}\left(D^{1-\alpha_j}\tilde{c}_j(s)\right)^2\,.\end{aligned}$$

Let us denote $\psi_j(s)=D^{1-\alpha_j}\tilde{c}_j(s)$. By definition of the fractional integral, this is the inverse operator of the fractional derivative, i.e. $I^{1-\alpha}D^{1-\alpha}f(t)=f(t)$. The function $c_j(0,s)$ is then equal to $c_j(0,s)=I^{1-\alpha_j}\psi_j(s)=\tilde{c}_j(s)$. By definition of the left Riemann-Liouville derivative, we finally infer that

$$\partial_s c_j(0,s) \;=\; \frac{dI^{1-\alpha_j}\psi_j(s)}{ds}=D^{\alpha_j}\psi_j(s)\,.$$

This last relation allows us to obtain Equations (25) and (27).

■

In numerical illustrations, we may think to compute the mgf with the discrete approximation proposed in Propositions 3.1 or 3.3. Nevertheless, this approach implies solving PDE's for $a_j(.,.)$ and $c_j(.,.)$, functions of $m_k^{(j)}$ that tends to infinity when the granularity of the partition $\mathcal{E}^{(n)}$ increases. This is a cause of numerical instability that makes difficult the computations of $a_j(.,.)$ and $c_j(.,.)$. A more reliable method consists to calculate the functions $\psi_j(t)$, $c_j(0,t)$ and $a_j(0,t)$ such as defined in Proposition 4.1. Since $D_0^\alpha I_0^\alpha f(t) = f(t)$, the fractional integral of Equation (25) provides us the following expression for ψ_j ,

$$\psi_j(t) \;=\; \int_0^t \frac{(t-s)^{\alpha_j-1}}{\Gamma(\alpha_j)} \left((\boldsymbol{\omega}_1 + \boldsymbol{\varphi}(\boldsymbol{\omega}_2) - \mathbf{1}_m)^\top \Phi_{.,j} - \kappa_j \psi_j(s) + \frac{1}{2}\sigma_j^2 \psi_j(s)^2 \right) ds \,,$$

that we discretize. We choose a time step, Δ and denote $t_k = k\,\Delta$ for $k = 0, ..., n_t$ where $n_t = \left\lfloor \frac{t}{\Delta} \right\rfloor$. To ligthen developments, we denote by $\psi_j(k)$ the approached value of ψ_j at time t_k, computed with the recursion

$$\psi_j(k) = \sum_{l=0}^{k-1} \frac{(t_k - t_l)^{\alpha_j-1}}{\Gamma(\alpha_j)} \left((\boldsymbol{\omega}_1 + \boldsymbol{\varphi}(\boldsymbol{\omega}_2) - \mathbf{1}_m)^\top \Phi_{.,j} - \kappa_j \psi_j(l) + \frac{1}{2}\sigma_j^2 \psi_j(l)^2 \right) \Delta \,, \tag{30}$$

for $k = 1, ..., n_t$ and an initial value $\psi_j(0) = 0$. As $c_j(0,t) = I^{1-\alpha_j}\psi_j(t)$ and $D^{\alpha_j}\psi_j(t) = \frac{dI^{1-\alpha_j}\psi_j(t)}{dt}$, we approach $c_j(0, t_k)$ by

$$c_j(k) \;=\; \sum_{l=0}^{k-1} \left((\boldsymbol{\omega}_1 + \boldsymbol{\varphi}(\boldsymbol{\omega}_2) - \mathbf{1}_m)^\top \Phi_{.,j} - \kappa_j \psi_j(l) + \frac{1}{2}\sigma_j^2 \psi_j(l)^2 \right) \Delta \,. \tag{31}$$

On the other hand, the function $a_j(0, t_k)$ is calculated from Equation (27) as the following sum

$$a_j(k) \;=\; \sum_{l=0}^{k-1} \left(\kappa_j \theta_j \psi_j(l)\right) \Delta \,. \tag{32}$$

We will see in Section 7 how to retrieve the pdf's of claim processes by inverting the mgf with a Discrete Fourier transform. But before, we detail an econometric technique used for filtering the sample path of intensities from observed claim processes.

5 Particle filtering

In practise, we do not directly observe the intensities of claims and we then need to develop a filter to guess their most likely sample paths. This section proposes a filtering technique based on Monte-Carlo simulations that also estimate the log-likelihood.

We consider a sample of discrete observations of claim processes. The interval of time between two observations is noted Δ and the times of sampling are $\{t_0, t_1, ..., t_T\}$. We adopt the notations $\lambda_k^{(j)} = \lambda_{t_k}^{(j)}$ for $j = 1, ..., m$, $X_k^{(i)} = X_{t_k}^{(i)}$ for $i = 1, ..., p$ and $\boldsymbol{X}_k = \{X_k^{(1)}, ..., X_k^{(p)}\}$. The realizations of $X_k^{(i)}$ are denoted by $x_k^{(i)}$ and stored in a vector $\boldsymbol{x}_k$. Over the interval $[t_k, t_{k+1}]$, the number of claims of the j^{th} category is Poisson distributed with a parameter

$\lambda_k^{(j)}\Delta = \Phi_{j,.}\boldsymbol{X}_k\,\Delta$. The dynamics of rough factors, (5) is approached by:

$$X_{k+1}^{(j)} = X_0^{(j)} + \sum_{i=0}^{k} \frac{(t_{k+1}-t_i)^{\alpha_j-1}\,\kappa_j\left(\theta_j - X_i^{(j)}\right)\Delta}{\Gamma(\alpha_j)} + \sum_{i=0}^{k} \frac{(t_{k+1}-t_i)^{\alpha_j-1}}{\Gamma(\alpha_j)}\sigma_j\sqrt{X_i^{(j)}}\,\Delta W_{i+1}^{(j)}\ ,\ j=1,...,p \tag{33}$$

where $\Delta W_{i+1}^{(j)} = W_{t_{i+1}}^{(j)} - W_{t_i}^{(j)}$. We note the set of parameters $\boldsymbol{\theta} = \{\alpha_j, \kappa_j, \theta_j, \sigma_j\}$ and it is assumed to be known in this section. The particle filter estimates the most likely sample path of the rough processes.

We denote by $\Delta w_i^{(j)}$ the realizations of $\Delta W_i^{(j)}$ and $\Delta\boldsymbol{w}_i$, $\Delta\boldsymbol{W}_i$ the corresponding vectors. The information $\boldsymbol{X}_i = \boldsymbol{x}_i$ and $\Delta W_i = \Delta\boldsymbol{w}_i$ for $i = 1, ..., k$ is stored in a "particle", noted $\boldsymbol{u}_k$. As intensities depend on their past realizations, we keep track of the whole sample path of rough factors and of Brownian increments.

The sample of claim counts of the j^{th} process over the T sub-intervals, is denoted by $\boldsymbol{n}^{(j)} = \{n_1^{(j)}, n_2^{(j)}, ..., n_T^{(j)}\}$ and $\boldsymbol{n}_k = \{n_k^{(1)}, ..., n_k^{(p)}\}$ is the number of claims over $[t_k, t_{k+1}]$. The time series of $\boldsymbol{n}_i$ from $i = 1$ up to k is noted $\boldsymbol{n}_{1:k}$.

The density of the "measurement" $f(\boldsymbol{n}_k|\boldsymbol{u}_k)$, conditionally to the information in the particle, is a product of Poisson density:

$$\begin{aligned} f(\boldsymbol{n}_k|\boldsymbol{u}_k) &= \prod_{j=1}^{m} P\left(n_k^{(j)}\,|\,\Phi_{j,.}\boldsymbol{x}_k\,\Delta\right) \\ &= \prod_{j=1}^{m} \frac{(\Phi_{j,.}\boldsymbol{x}_k\,\Delta)^{n_k^{(j)}}}{n_k^{(j)}!}\exp\left(-\Phi_{j,.}\boldsymbol{x}_k\,\Delta\right) \end{aligned}$$

On the other hand, the transition density $f(\boldsymbol{u}_{k+1}\,|\,\boldsymbol{u}_k)$ is simulated with Equation (33). The pdf of $\boldsymbol{x}_0$ is $f(\boldsymbol{x}_0)$. The posterior distribution of $\boldsymbol{u}_j$ conditionally to the available information at t_j is then rewritten as follows:

$$f(\boldsymbol{u}_k\,|\,\boldsymbol{n}_{1:k}) = \frac{f(\boldsymbol{n}_k\,|\,\boldsymbol{u}_k)}{\int f(\boldsymbol{n}_k|\boldsymbol{u}_k) f(\boldsymbol{u}_k\,|\,\boldsymbol{n}_{1:k-1}) d\boldsymbol{u}_j} f(\boldsymbol{u}_k\,|\,\boldsymbol{n}_{1:k-1})\,, \tag{34}$$

where

$$f(\boldsymbol{u}_k\,|\,\boldsymbol{n}_{1:k-1}) = \int f(\boldsymbol{u}_k\,|\,\boldsymbol{u}_{k-1}) f(\boldsymbol{u}_{k-1}\,|\,\boldsymbol{n}_{1:k-1}) d\boldsymbol{u}_{k-1}\,. \tag{35}$$

The calculation of $f(\boldsymbol{u}_k\,|\,\boldsymbol{n}_{1:k})$ is performed in three steps. In a first prediction step, we approach $f(\boldsymbol{u}_k\,|\,\boldsymbol{n}_{1:k-1})$ by simulations. In the correction step, we calculate probabilities $f(\boldsymbol{u}_k\,|\,\boldsymbol{n}_{1:k})$ using the equation (34) where the integral is replaced by a Monte-Carlo simulation, of N "particles". In the third step, we resample particles to keep track of the most likely sample paths. The particle filter is presented in Algorithm 1.

Algorithm 1 Particle filtering of rough factors.

Initial step :

draw N values of $\boldsymbol{x}_0^{(i)}$ for $i = 1, \ldots, N$, from an initial distribution $f(\boldsymbol{x}_0)$.

Main procedure :

For $k = 1$ to maximum epoch, T

Prediction step

Draw a sample $\Delta \boldsymbol{w}_k^{(i)}$from p r.v. $N(0, \sqrt{\Delta})$, $i = 1, ...N$.

Update $\boldsymbol{x}_k^{(i)}$ using the relation

$$\boldsymbol{x}_k^{(i)} = \boldsymbol{x}_0^{(i)} + \sum_{l=0}^{k-1} \frac{(t_k - t_l)^{\boldsymbol{\alpha}-1} \odot \boldsymbol{\kappa} \odot \left(\boldsymbol{\theta} - \boldsymbol{x}_l^{(i)}\right) \Delta}{\Gamma(\boldsymbol{\alpha})} + \sum_{l=0}^{k-1} \frac{(t_{k+1} - t_l)^{\boldsymbol{\alpha}-1}}{\Gamma(\boldsymbol{\alpha})} \odot \boldsymbol{\sigma} \odot \sqrt{\boldsymbol{x}_l^{(i)} \odot} \, \Delta \boldsymbol{w}_{l+1}^{(i)} \, , \; i = 1, ..., N \tag{36}$$

where $\odot$ is the elementwise product.

Correction step:

The i^{th} "particle" $\boldsymbol{u}_k^{(i)} = \left(\boldsymbol{x}_l^{(i)}, \Delta \boldsymbol{w}_l^{(i)}\right)_{l=1:k}$ has a probability of occurence

$$p_k^{(i)} = \frac{f(\boldsymbol{n}_k \,|\, \boldsymbol{u}_k^{(i)})}{\sum_{i=1:N} f(\boldsymbol{n}_k \,|\, \boldsymbol{u}_k^{(i)})} \, ,$$

where

$$f(\boldsymbol{n}_k \,|\, \boldsymbol{u}_k^{(i)}) = \prod_{j=1}^{m} \frac{\left(\Phi_{j,.} \boldsymbol{x}_k^{(i)} \, \Delta\right)^{n_k^{(j)}}}{n_k^{(j)}!} \exp\left(-\Phi_{j,.} \boldsymbol{x}_k^{(i)} \, \Delta\right)$$

Resampling step:

Resample with replacement N particles according to
the importance weights $p_j^{(i)}$.

The new importance weights are set to $p_j^{(i)} = \frac{1}{N}$.

End loop on epochs

The filtered k^{th} factor for the period j is computed as the sum of $\boldsymbol{x}_k^{(i)}$ contained in particles weigthed by their probability of occurence:

$$\widehat{\boldsymbol{x}}_k = \mathbb{E}\left(\boldsymbol{x}_k \,|\, \boldsymbol{n}_{1:k}\right) = \sum_{i=1}^{N} \boldsymbol{x}_k^{(i)} p_k^{(i)} \, .$$

The log-likelihood of the whole sample is approached before resampling by the sum:

$$\log f(\boldsymbol{n}|\boldsymbol{\theta}) \;\; = \;\; \sum_{k=1}^{T} \log\left(\sum_{i=1}^{N} \frac{1}{N} f(\boldsymbol{n}_k \,|\, \boldsymbol{u}_k^{(i)})\right) \, . \tag{37}$$

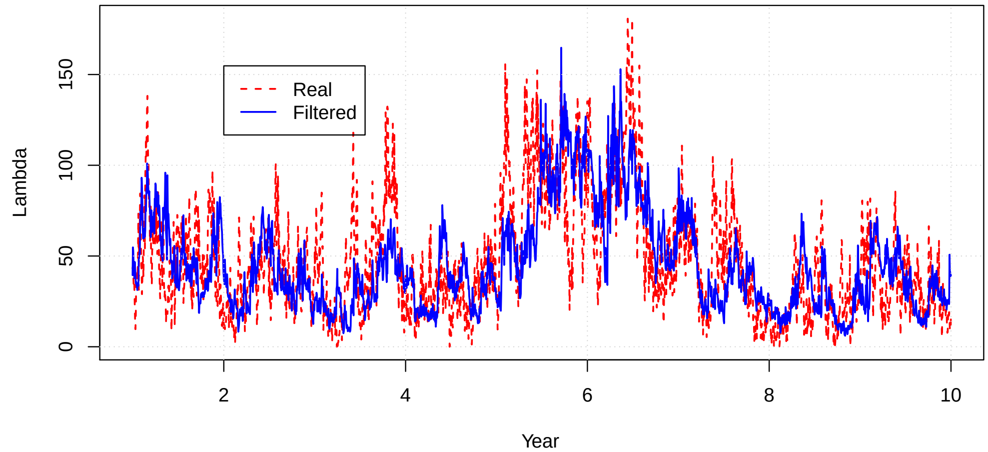

Figure 1: Comparison of simulated and filtered sample paths of λ_t, for a 1D claim process.

In practise, the update of $\boldsymbol{x}_k^{(i)}$ such as proposed in Equation (36) is computationally intensive. A less time consuming method consists to approach the variation of $\boldsymbol{x}_k^{(i)}$ with Equations (11) and (12) for a partitition $\mathcal{E}^{(n)}$ with a reasonable number of points of discretization.

To test the filter, we simulate a one dimensional claim process ($m = 1$) driven by a single rough process ($p = 1$). The chosen parameters are $\kappa = 0.8$, $\theta = 20$, $\sigma = 5$, $\Phi = 1$. The time horizon is 10 years with 250 steps per year. Figure 1 compares simulated and filtered sample paths of λ_t with $N = 50$ particles. This graph confirms the capacity of the particle filter to track the evolution of the unobservable intensity.

6 Estimation: a case study

We use the particle filter of the previous section for estimating a model by log-likelihood maximization. Nevertheless the log-likelihood being computed by simulations is noised which is harmful for the convergence of the optimization procedure. A first way to tackle this problem consists to work with a Markov Chain Monte-Carlo (MCMC) method. However, the convergence of this type of algorithm is sometimes hazardous since it depends on unknown prior and transition distributions of parameters. In this article, we opt for a simpler alternative that consists to run a few times Nelder-Mead algorithm and to select the set of parameters leading to the lowest average log-likelihoods (during the last iterations). We illustrate this procedure with the dataset from the Privacy Rights Clearinghouse[2] (PRC) that contains information about 8871 data breaches in USA since 2005. We focus on cyber-attacks by outside party and infections by malware from the 1/1/2014 to 31/12/2018. We consider two categories of sectors targeted by these attacks. The first one regroups healthcare, medical providers or medical Insurance services (MED). The second one gathers financial businesses (BSF), other

[2]https://www.privacyrights.org/data-breaches

businesses (BSO) and retail businesses (BSR). We refer the reader to Bessy-Roland et al. [4] for a detailed analysis of this dataset. We also cite Farkas et al. [12] who study this dataset with regression trees to identify criteria for claim classification. Over the considered period, 762 and 624 attacks were respectively reported for MED and BSF-O-R sectors. The evolution of weekly numbers of cyber-attacks between 2014 and 2018 is plotted in Figure 2. Notice that several events are reported on same days and that claim amounts are not available.

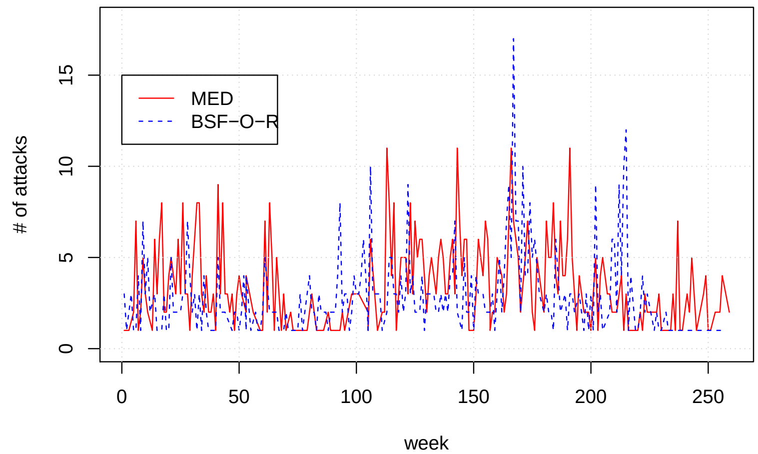

Figure 2: Weekly numbers of cyber-attacks in the MED and BSF-O-R sectors from 1/1/2014 to 31/12/2018.

We start our analysis by estimating 1 dimensional (1D) claim counting processes ($m = p = 1$) with a filter using N =300 particles. Tables 1 and 2 respectively report the parameters, log-likelihoods, AIC of 1D pure Poisson processes and of 1D rough Cox and pure Cox (such as defined by Equation (6)) processes. The AIC's clearly plead in favour of models with stochastic intensities. For the MED sector, considering a rough dynamic significantly reduces the AIC. For the BSF-O-R sector, log-likelihoods of 1D rough and non-rough models are comparable and the AIC favours the CIR dynamic since it counts one less parameter than the 1D rough model.

	Poisson processes	
	MED	BSF-O-R
$\lambda^{(j)}$	150.31	123.09
Log-Likelihood	-1663.07	-1453.03
AIC	3328.13	2908.06

Table 1: Parameter estimates, log-likelihood and AIC of Poisson processes fitted to cyber-attacks in the MED and BSF-O-R sectors.

Table 3 displays parameter estimates and goodness of fit statistics for bivariate claim processes. Both for rough and pure Cox processes, the 2D log-likelihoods are lower than the sum of their 1D counterparts. Furthermore, the lowest AIC is obtained with a rough Cox process. This confirms firstly the existence of contagion between cyber attacks targetting MED and other sectors. Secondly, we cannot exclude that frequencies of these attacks have rough dynamics.

	Rough Cox, 1D		Cox, 1D	
	MED	BSF-O-R	MED	BSF-O-R
κ	2.11	2.03	1.32	2.45
θ	143.36	93.27	150.63	92.34
σ	14.79	20.46	17.31	20.07
α	0.55	0.92	n.a.	n.a.
Log-Likelihood	-1579.54	-1361.27	-1590.21	-1361.15
AIC	3167.08	2730.54	3186.37	2716.30

Table 2: Parameter estimates, log-likelihood and AIC of 1D Rough and 1D Cox processes fitted to cyber-attacks in the MED and BSF-O-R sectors.

	Rough Cox, 2D		Cox, 2D	
	$X_t^{(1)}$	$X_t^{(2)}$	$X_t^{(1)}$	$X_t^{(2)}$
κ_j	2.25	2.14	1.55	1.82
θ_j	143.97	104.54	137.04	91.38
σ_j	12.97	24.24	18.37	21.93
α_j	0.55	0.92	n.a.	n.a.
$\phi_{1,2}$	0.1358		0.1134	
$\phi_{2,1}$	0.0836		0.1305	
$\phi_{1,1}$, $\phi_{2,2}$	1		1	
Log-Likelihood	2508.96		2517.60	
AIC	5037.92		5051.2	

Table 3: Parameter estimates, log-likelihood and AIC of 2D processes fitted to cyber-attacks in the MED and BSF-O-R sectors.

We conclude this section by presenting in Figure 3, the filtered intensities of MED and BSF-O-R claim counting processes. For this exercise, we run the filter with 300 particles for 1D rough, 2D rough and 2D non-rough processes. The upper plot reveals that the volatility of the MED intensity is higher in rough than in non-rough models. For the BSF-O-R sector, the intensities of attacks display similar sample paths whatever the chosen dynamic. In the next Section, we report additional statistics about aggregated claim processes over 1 year, by inverting their mgf.

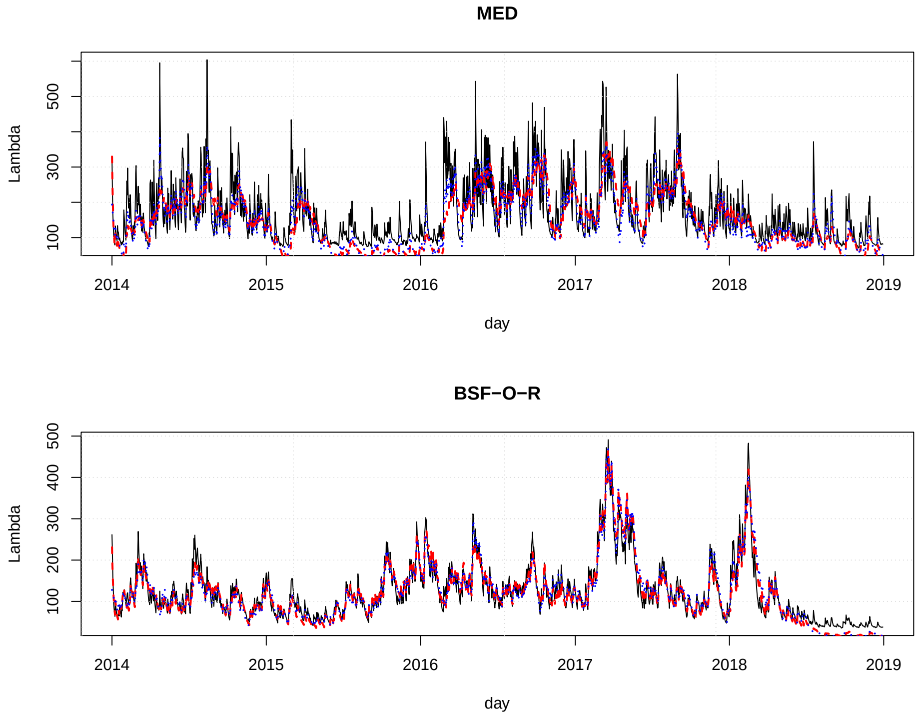

Figure 3: Filtered intensities for MED and BSF-O-R cyber attacks from the 1/1/2014 to 31/12/2018.

7 Probability density functions by FFT

We have found in Section 4, the moment generating function of a multivariate claim process with rough intensities. We exploit this result to compute the joint and marginal probability density functions (pdf's) of cyber claim processes and to report additional statistics. Our approach is based on a discrete fast Fourier's transform (DFFT). It roughly consists to invert the characteristic function of the claim process, that is the mgf valued on the imaginary axis.

Let us denote the characteristic function of claim processes by $\Upsilon_s(i\boldsymbol{\omega}) = \mathbb{E}\left(e^{i\boldsymbol{\omega}^\top \boldsymbol{L}_s} \,|\, \mathcal{F}_0\right)$, that is also the inverse Fourier transform of the multivariate probability density function (pdf) $f_s(\boldsymbol{x})$ of $\boldsymbol{L}_s|\mathcal{F}_0$. Therefore, this density can be retrieved by computing the following multiple integrals (the Fouriertransform, $\mathcal{F}[.]$, of $\Upsilon_s(.)$):

$$\begin{aligned} f_s(\boldsymbol{x}) &= \frac{1}{(2\pi)^m}\mathcal{F}[\Upsilon_s(i\boldsymbol{\omega})](\boldsymbol{x}) \\ &= \frac{1}{(2\pi)^m}\int_{-\infty}^{+\infty}...\int_{-\infty}^{+\infty}\Upsilon_s(i\boldsymbol{\omega})e^{-i\boldsymbol{\omega}^\top\boldsymbol{x}}d\omega_1...d\omega_m\,. \end{aligned} \tag{38}$$

The calculation of this multiple integral is computationally intensive but it may be speed up if we discretize it in a compatible expression with the DFFT, as presented in the next proposition.

Proposition 7.1. *Let M be the number of steps used in the Discrete Fast Fourier Transform (DFFT) and $\Delta_x = \frac{x_{max}}{M}$, be the step of discretization. Let us denote $\Delta_\omega = \frac{2\pi}{M\,\Delta_x}$ and*

$$\boldsymbol{\omega}_{j_1,j_2,\dots,j_m} = \left(-\frac{M}{2}\Delta_\omega + (j_1-1)\Delta_\omega, -\frac{M}{2}\Delta_\omega + (j_2-1)\Delta_\omega, \dots, -\frac{M}{2}\Delta_\omega + (j_m-1)\Delta_\omega\right)$$

for $j_1,\dots,j_m \in \{1,\dots,M+1\}$. The values of $f_s(.)$ at points

$$\boldsymbol{x}_{k_1,k_2,\dots,k_m} = ((k_1-1)\Delta_x\,,\,(k_2-1)\Delta_x\,,\,\dots,(k_m-1)\Delta_x)$$

for $k_1,\dots,k_m \in \{1,\dots,M\}$ are approached by

$$\begin{aligned} f_s(\boldsymbol{x}_{k_1,\dots,k_m}) &= (\Delta_\omega)^m \sum_{j_1=1}^{M+1}\sum_{j_2=1}^{M+1}\dots\sum_{j_m=1}^{M+1} \delta_{j_1,j_2,\dots,j_m}\Upsilon_s\left(i(\boldsymbol{\omega}_{j_1,j_2,\dots,j_m})\right) \\ &\quad \times \exp\left(i\sum_{l=1}^{m}((k_l-1)\pi)\right) \times \exp\left(-i\sum_{l=1}^{m}(k_l-1)(j_l-1)\frac{2\pi}{M}\right) \end{aligned} \tag{39}$$

where$\Upsilon_s(i\boldsymbol{\omega}) = \mathbb{E}\left(e^{i\,\boldsymbol{\omega}^\top \boldsymbol{L}_s}\,|\,\mathcal{F}_t\right)$ *is defined by equation (26) and*

$$\delta_{j_1,j_2,\dots,j_m} = \left(\frac{1}{2}\right)^{(1_{\{j_1=1\}}+\dots+1_{\{j_m=1\}})}(1-1_{\{j_1\neq 1,\dots,j_m\neq 1\}}) + 1_{\{j_1\neq 1,\dots,j_m\neq 1\}}\,.$$

The proof is standard and may be found in e.g. Hainaut ([14]). The expression (39) emphasizes that $f_s(\boldsymbol{x}_{k_1,\dots,k_m})$ is computable with a standard DFFT algorithm applied to $(\Delta_\omega)^m\,\delta_{j_1,j_2,\dots,j_m}\Upsilon_s\left(i(\boldsymbol{\omega}_{j_1,j_2,\dots,j_m})\right)\exp\left(i\sum_{l=1}^{m}((k_l-1)\pi)\right)$ valued on the meshgrid $j_1,\dots,j_m \in \{1,\dots,M+1\}$.

The dataset does not report claim costs. In order to illustrate this section, we have assumed that claim costs, $J^{(j)}$, are exponential random variables with parameters $\rho^{(j)} = 1$ for $j = 1$ (MED) and $j = 2$ (BSF-O-R). The $L_t^{(j)}$'s may then be interpreted as claim counting processes (at least on average). The left upper plot of Figure 4 shows the joint pdf of $L_t^{(MED)}$ and $L_t^{(BSF)}$over a one year period (with parameters of Table 3). The equations (31), (32) and (30) are numerically solved by backward iterations with a time step of 1/200. The bivariate DFFT is run with $M = 2^6$ and we set $X_0^{(j)} = \theta_j$.

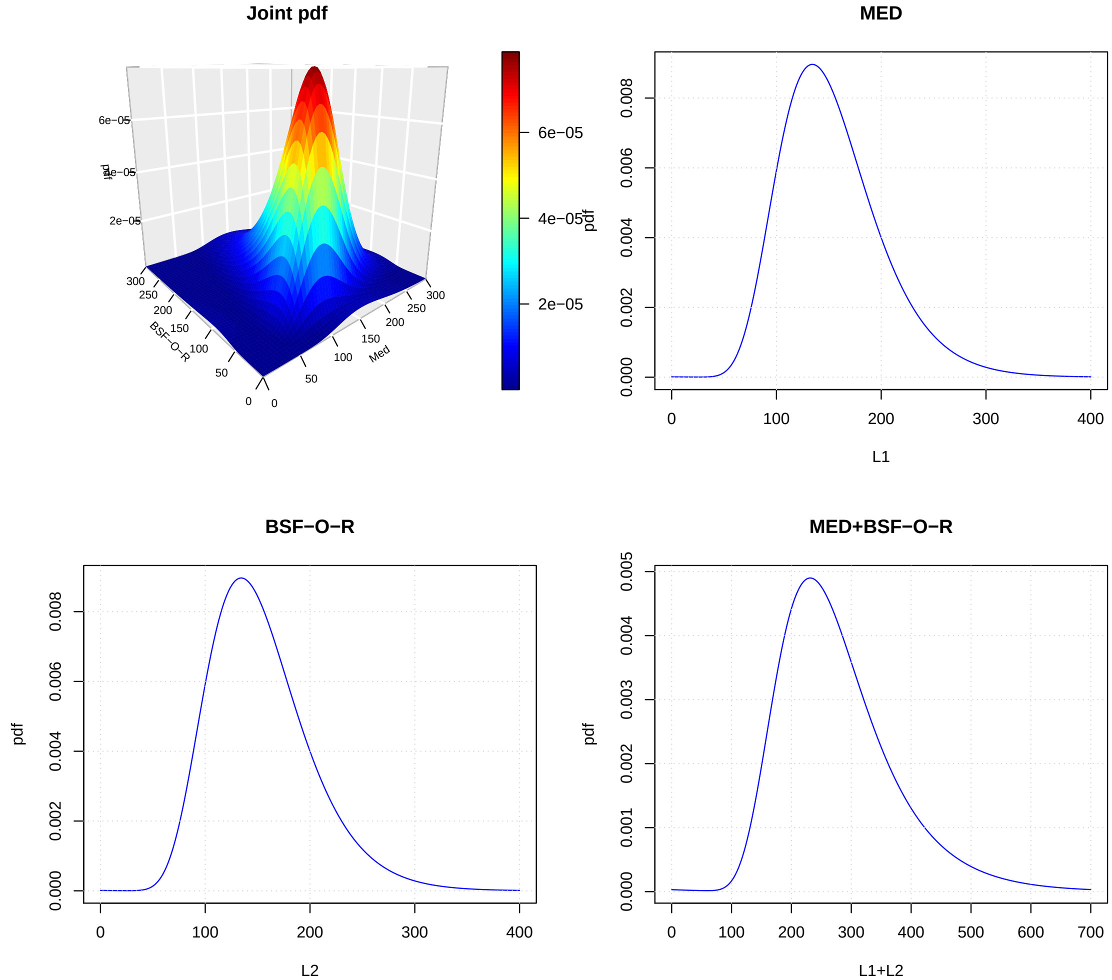

Figure 4: Left upper plot: joint pdf of $L_t^{(MED)}$ and $L_t^{(BSF)}$, over 1 year. Other plots: marginal pdf's and pdf of the sum.

In practice, computing the joint pdf of more than 2 claim processes is time consuming. Nevertheless, in high dimension, it is still possible to calculate the marginal pdf's or the pdf of aggregated claim processes with a one dimensional Fourier transform. Let $\boldsymbol{\chi}$ be a m-vector taking its value in the set of orthonormal basis vectors $\{\boldsymbol{e}_1, ...\boldsymbol{e}_m\}$ of $\mathbb{R}^m$ or being equal to the unit vector $\boldsymbol{e} = (1, ..., 1)^\top$. We denote by $f_s^{\boldsymbol{\chi}}(.)$ the univariate pdf of the linear combination $\boldsymbol{\chi}^\top \boldsymbol{L}_s | \mathcal{F}_0$. This density is equal to the following univariate Fourier transform:

$$f_s^{\boldsymbol{\chi}}(x) \quad = \quad \frac{1}{2\pi} \int_{-\infty}^{+\infty} \Upsilon_s(i\,\omega\,\boldsymbol{\chi}) e^{-i\omega x} d\omega \,.$$

From the previous proposition, this integral can be discretized in a compatible expression with the one dimensional DFFT as detailed in the next corollary.

Corollary 7.2. *Let M be the number of steps used in the Discrete Fast Fourier Transform (DFFT) and $\Delta_x = \frac{x_{max}}{M}$, be the step of discretization. Let us denote $\Delta_\omega = \frac{2\pi}{M\,\Delta_x}$ and $\omega_j = -\frac{M}{2}\Delta_\omega + (j-1)\Delta_\omega$ for $j = 1, ..., M+1$. The values of $f_s^{\boldsymbol{\chi}}(.)$ at points $x_k = (k-1)\Delta_x$ for $k = 1, ..., M$ are approached by*

$$\begin{aligned} f_s^{\boldsymbol{\chi}}(x_k) &= \Delta_\omega \sum_{j=1}^{M+1} \delta_j \Upsilon_{t,s}\left(i(\omega_j\, \boldsymbol{\chi})\right) \exp\left(i\left((k-1)\pi\right)\right) \\ &\quad \times \exp\left(-i(k-1)(j-1)\frac{2\pi}{M}\right) , \end{aligned} \tag{40}$$

where$\delta_j = \left(\frac{1}{2}\right)^{1_{\{j_1=1\}}} + 1_{\{j\neq 1\}}$.

Marginal and aggregated pdf's are then computable in a reasonable time (less than one minute for $M = 2^8$ on a standard laptop) with a 1D DFFT applied to

$$\Delta_\omega \delta_j \Upsilon_s\left(i(\omega_j\, \boldsymbol{\chi})\right) \exp\left(i\left((k-1)\pi\right)\right) .$$

The upper right and lower left, right plots of Figure 4 respectively present the pdf of $L_t^{(MED)}$, $L_t^{(BSF)}$ and $L_t^{(MED)}+L_t^{(BSF)}$over a period of one year. These pdf's are obtained with a 1D DFFT and 2^8 discretization steps. Parameters are those of the 2D model in Table 3. The expectations, standard deviations (st. dev.), 5% and 95% percentiles of these distributions are reported in Table 4. The same statistics computed with parameters of the 2D non-rough process are reported in Table 5. Both models have similar one-year expectations. We observe that the marginal and total variances of the 2D Cox claim processes is higher than those computed with the 2D rough model. This is an interesting observation. Despite rough intensities have more chaotic sample paths than their Brownian counterpart, using a rough dynamic does not necessary implies an increase of volatility of aggregated claims but improves the goodness of fit.

2D rough Cox model			
	MED, $L_t^{(MED)}$	BSF-O-R, $L_t^{(BSF)}$	$L_t^{(MED)}+L_t^{(BSF)}$
Expectation	153.38	121.08	276.47
St. dev.	48.57	68.63	95.52
5% perc.	84.71	40.78	148.24
95% perc.	243.14	263.53	458.43
x_{max}	400	400	700
M	2^8	2^8	2^8

Table 4: Rough 2D model. Expectations, standard deviations (st. dev.), 5% and 95% percentiles of claim processes $L_t^{(MED)}$, $L_t^{(BSF)}$ and $L_t^{(MED)}+L_t^{(BSF)}$. x_{max} and M are the DFFT parameters.

2D Cox model			
	MED	BSF-O-R	TOTAL
Expectation	153.26	113.36	263.77
St. dev.	78.57	72.63	114.69
5% perc.	54.90	32.94	109.80
95% perc.	304.71	258.04	483.14
x_{max}	400	400	700
M	2^8	2^8	2^8

Table 5: Non-rough 2D model. Expectations, standard deviations (st. dev.), 5% and 95% percentiles of claim processes $L_t^{(MED)}$, $L_t^{(BSF)}$ and $L_t^{(MED)}+L_t^{(BSF)}$. x_{max} and M are the DFFT parameters.

8 Conclusions

To the best of our knowledge, this article is one of the first to study a multivariate claim process driven by rough Brownian motions. Since intensities of claims counting processes are not semi-martingales, we cannot rely anymore on standard Itô calculus to study their properties. Nevertheless, rough factors admit an infinite dimensional Markov representation that we approximate by discretization in a similar way to Abi Jaber and El Euch ([2]). In this discrete setting, the moment generating function of claim processes is computable by solving backward ODE's. As this mgf does not admit any limit when the number of discretization steps increases, we first reformulate it in terms of forward ODE's. Next we show that this discrete forward approximation of the mgf admits a limit involving fractional differential equations. The mgf of claim processes present similarities with the one of the rough Heston model obtained by El Euch and Rosenbaum ([11]) by considering the limit of nearly unstable Hawkes processes. Our method for establishing such a result is nevertheless simpler and novel since it is based on a discrete approximation of Riemann-Liouville derivatives.

In practise, the calibration of a rough model is a challenging task since intensities of claims counting processes are not directly observable. To tackle this problem, we propose a procedure to filter their most likely sample paths from observed claim processes. This method, called particle filter, is based on Monte-Carlo simulations and can also serves for estimation. We illustrate this by fitting 1D and 2D models to time-series of cyber-attacks in the USA, targeting medical and other services from begin of 2014 to end of 2018. We detail and apply the method for computing the joint and marginal pdf's of claim processes by DFFT. This allows us to compare moments and percentiles to these of a standard Cox model. We conclude that rough models provide a better fit than their non-rough equivalents. We also notice that even if rough intensities have more chaotic sample paths than their Brownian counterpart, using a rough dynamic does not necessary implies an increase of volatility of aggregated claims processes.

This article opens the way to further research. Firstly, the proposed model is not designed for managing negative correlation between counting processes because intensities are positive linear combinations of rough factors. Secondly, we may want to introduce correlation between rough factors. Another track is to consider hybrid models mixing rough and non-rough factors.

Acknowledgment

This work was supported by the "Fonds de la Recherche Scientifique" - FNRS under Grant n° 33658713.

References

[1] Abi Jaber E., Larsson M., Pulido S. 2019. Affine volterra processes, Annals of Applied Probability 29 (5), 3155–3200.

[2] Abi Jaber, E., El Euch O. 2019. Multi-factor approximation of rough volatility models. SIAM Journal of Financial Mathematics , 10(2), 309–349.

[3] Bayer C., Friz P., Gatheral J. 2016. Pricing under rough volatility. Quantitative Finance, 16 (6), 887–904.

[4] Bessy-Roland Y., Boumezoued A., Hillairet C. 2020. Multivariate Hawkes process for cyber insurance. Annals of Actuarial Sciences 15 (1), pp. 14-39.

[5] Cox D.R., 1955. Some statistical methods connected with series of events. J. R. Statist. Soc. Ser. B 17, 129-164.

[6] Cox J.C., Ingersoll J.E. , Ross S.A. 1985. A Theory of the Term Structure of Interest Rates, Econometrica, 53, pp. 385–407.

[7] Dupret J.L., Barbarin J., Hainaut D. 2021. Impact of rough stochastic volatility models on long-term life insurance pricing. Forthcoming in European Actuarial Journal.

[8] Dupret J.L., Hainaut D. 2021. Portfolio insurance under rough volatility and Volterra processes. Forthcoming in International Journal of Theoretical and Applied Finance.

[9] El Euch O., Gatheral J., Rosenbaum M. 2019. Roughening heston. Risks, 84–89.

[10] El Euch, O., Rosenbaum, M. 2018. Perfect hedging in rough heston models. The Annals of Applied Probability 28(6), 3813–3856.

[11] El Euch O., Rosenbaum M. 2019. The characteristic function of rough heston models, Mathematical Finance 29 (1), 3–38.

[12] Farkas S., Lopez O., Thomas M. 2021. Cyber claim analysis using Generalized Pareto regression trees with applications to insurance. Insurance: Mathematics and Economics 98, 92-105.

[13] Gatheral J. Jaisson T., Rosenbaum M. 2018. Volatility is rough, Quantitative Finance 18 (6), 933–949.

[14] Hainaut D. 2021. Moment generating function of non-Markov self-excited claims processes. Insurance: Mathematics & Economics, 101 (B), 406-424.

[15] Jumarie G. 2005. Merton's model of optimal portfolio in a Black-Scholes Market driven by a fractional Brownian motion with short-range dependence. Insurance: Mathematics & Economics, 37 (3), 585-598

[16] Kolmogorov A., 1940. Wienersche Spiralen und einige andere interessante kurven im Hilbertschen raum, C. R. (Doklady) Acad. Sci. URSS (N.S.), 26, 115- 118

[17] MandelBrot B., Van Ness J.W. 1968. Fractional Brownian motions, Fractional Noises and Applications. SIAM Review, 10 (4), 422-437.